



# A new linear form analysis of Redlich–Peterson isotherm equation for the adsorptions of dyes

Feng-Chin Wu<sup>a</sup>, Bing-Lan Liu<sup>b</sup>, Keng-Tung Wu<sup>c</sup>, Ru-Ling Tseng<sup>d,\*</sup>

<sup>a</sup> Department of Chemical Engineering, National United University, Miao-Li 360, Taiwan

<sup>b</sup> Department of Applied Chemistry, Chaoyang University of Technology, Taichung 413, Taiwan

<sup>c</sup> Department of Forestry, National Chung Hsing University, Taichung 402, Taiwan

<sup>d</sup> Department of Safety, Health and Environmental Engineering, National United University, No. 1, Lien Da, Kung-Ching Li, Miao-Li 360, Taiwan

## ARTICLE INFO

### Article history:

Received 23 August 2009

Received in revised form 1 March 2010

Accepted 1 March 2010

### Keywords:

Activated carbon

Redlich–Peterson equation

Adsorption isotherm

Dyes

## ABSTRACT

Many papers report that accuracy of the Redlich–Peterson (R–P) isotherm equation (three parameters) is higher than those of Langmuir and Freundlich isotherm equations (two parameters). This paper first explains why the accuracy of the R–P isotherm equation is equal to or higher than that of two parameters isotherm equations. This study suggests a new exponential linear equation with exponent variable  $\alpha$ , and solves the most suitable  $\alpha$  value with the aid of Microsoft Excel and Sigma Plot 9.0. This exponential method is quick, simple, and accurate for fitting the R–P isotherm equation to experimental data sets of adsorption systems compared with a logarithmical linear form frequently used previously. This investigation prepares four kinds of pistachio shell activated carbons with various doses of NaOH for studying isotherm equilibrium adsorptions of three dyes. The R–P isotherm equation best fit adsorption system data sets studied in this work.

© 2010 Published by Elsevier B.V.

## 1. Introduction

Redlich and Peterson suggested a three parameter adsorption isotherm equation [1] in 1959, unanimously called the Redlich–Peterson (R–P) isotherm equation (or model). The equation amends inaccuracies of two parameter Langmuir and Freundlich isotherm equations in some adsorption systems. In the literature survey, thirty papers reported the R–P equation was more accurate than the Langmuir and Freundlich equation in describing adsorption systems [2–31]; twelve papers reported that both R–P and Langmuir isotherm equations had equally high accuracy [32–43] because when  $\alpha$  value in the R–P equation equals 1, its form is the same as the Langmuir equation. Three papers additionally reported that both R–P and Freundlich isotherm equations had equally high accuracy [44–46] because when the constant value of the R–P equation is large enough, its form is the same as the Freundlich equation (proved later in this text); but the same papers reported Langmuir isotherm equation accuracy was higher than the R–P isotherm equation (not shown). These results are doubtful because when  $\alpha$  value is adjusted to equal 1, both equations are the same and both accuracies should be the same. Another papers reported Freundlich isotherm equation accuracy was higher

than the R–P isotherm equation (not shown). This cannot be correct either.

The poorer accuracy of the R–P isotherm equation reported in much of the literature is due to poor fitting methods. Therefore, this study suggests a simple, accurate operating method of the Redlich–Peterson isotherm equation. The adsorption of three dyes (BB1, MB, and AB74) used activated carbon prepared from pistachio shells with NaOH activation was carried out in this investigation. The results show the superiority of the Redlich–Peterson isotherm equation for describing adsorption systems by comparing R–P, Langmuir, and Freundlich isotherm equations and a suitable  $\alpha$  value range. The characteristic curve of the dimensionless R–P equation form explains the wide application of this equation.

## 2. Principle

### 2.1. Linear form of R–P isotherm equation

The R–P isotherm equation is expressed as

$$q_e = \frac{q'_{mon} b_{RP} C_e}{1 + b_{RP} C_e^\alpha} \quad (1)$$

where  $q'_{mon}$  and  $b_{RP}$  are parameters of the R–P isotherm equation. Two linear forms of Eq. (1) can be obtained by transformation as

\* Corresponding author. Tel.: +886 37 381775; fax: +886 37 333187.  
E-mail address: [trl@nuu.edu.tw](mailto:trl@nuu.edu.tw) (R.-L. Tseng).

and

$$\ln \left( b_{RP} q'_{mon} \frac{C_e}{q_e} - 1 \right) = \ln b_{RP} + \alpha \ln C_e \quad (2)$$

and

$$\frac{C_e}{q_e} = \frac{1}{b_{RP} q'_{mon}} + \left( \frac{1}{q'_{mon}} \right) C_e^\alpha \quad (3)$$

The logarithmic linear form of Eq. (2) was adopted by many researchers [6,8,11,13,19,24,25,27,28,30,32,36–38,43]. For fitting Eq. (2) to the experimental data to obtain a linear plot of  $\ln(b_{RP} q'_{mon} (C_e/q_e) - 1)$  vs.  $\ln C_e$ , various constant ( $b_{RP} q'_{mon}$ ) values must be tried before the optimum line is obtained. After obtaining the optimum line, calculate the constants of Eq. (2). The range of  $b_{RP} q'_{mon}$  values is wide, from 0.01 to several hundred, so it is not easy to obtain the correct value. Eq. (3) is the exponential linear form obtained by plotting  $C_e/q_e$  vs.  $C_e^\alpha$ . By trial and error, this study adopted an  $\alpha$  value for the optimum line. In the specific range,  $\alpha$  values are limited and it is easy to obtain the correct value (to be proved later). Another similar form of Eq. (3) has appeared in a few papers [17,47–49].

## 2.2. Special conditions of R–P isotherm equation

When  $\alpha = 1$ , it is the same as the Langmuir isotherm equation.

$$\frac{C_e}{q_e} = \frac{1}{K_L q_{mon}} + \left( \frac{1}{q_{mon}} \right) C_e \quad (4)$$

where  $b_{RP}$  of Eq. (3) equals  $K_L$  of Eq. (4), and  $q'_{mon}$  equals  $q_{mon}$ . When  $1/b_{RP} q'_{mon} = 0$ , it is the same as the Freundlich isotherm equation, that is

$$q_e = K_F C_e^{1/n} \quad (5)$$

where  $1/q'_{mon}$  of Eq. (3) equals  $K_F$  of Eq. (5), and  $\alpha$  equals  $1/n$ . Usually,  $1/b_{RP} q'_{mon}$  is not equal to 0, and  $q'_{mon}$  is constant, so only when  $b_{RP}$  is large enough, is the result of the R–P equation close to the Freundlich equation. When  $\alpha = 0$ , Eq. (1) can be written as

$$q_e = \frac{q'_{mon} b_{RP} C_e}{1 + b_{RP}} \quad (6)$$

Eq. (6) is the same as Henry's law equation.

## 2.3. Characteristic curves of R–P isotherm equation

Eq. (3) can be rewritten as:

$$\frac{C_{ref}}{q_{ref}} = \frac{1}{b_{RP} q'_{mon}} + \left( \frac{1}{q'_{mon}} \right) C_{ref}^\alpha \quad (7)$$

where  $C_{ref}$  is the highest equilibrium concentration of the adsorption system, and  $q_{ref}$  is the equilibrium adsorption amount at  $C_{ref}$ . When Eq. (7) is divided by Eq. (3), it yields

$$\frac{q_e}{q_{ref}} = \left( \frac{C_e}{C_{ref}} \right) \frac{(1/b_{RP} C_{ref}^\alpha) + 1}{(1/b_{RP} C_{ref}^\alpha) + (C_e/C_{ref})^\alpha} \quad (8)$$

Eq. (8) is the dimensionless form of the R–P isotherm equation. Fig. 1(a) and (b) depict plots of  $q_e/q_{ref}$  vs.  $C_e/C_{ref}$  with  $\alpha$  as a parameter for  $b_{RP} C_{ref}^\alpha = 2$  and 10, respectively. When  $\alpha = 1$ , the curve is the same as the curve in the Langmuir isotherm equation. The  $\alpha$  value modifies the curve. When  $\alpha$  value increases, curvature increases. Usually, the  $\alpha$  value reported in literature is less than 1 (proved later in this text). These low  $\alpha$  values mean their isotherm equation curves are milder than those of the Langmuir isotherm equation.

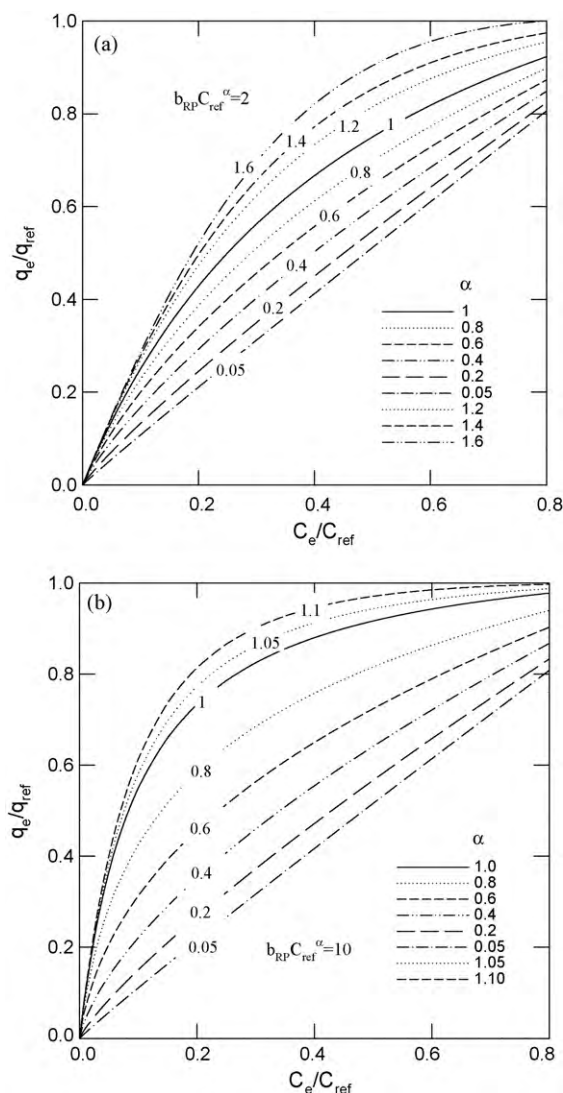


Fig. 1. Adsorption characteristic curves of dimensionless Redlich–Peterson isotherm equation (a)  $b_{RP} C_{ref}^\alpha = 2$  and (b)  $b_{RP} C_{ref}^\alpha = 10$ .

## 3. Materials and method

### 3.1. Preparation of the activated carbon

Pistachio shells were dried at 110 °C for more than 24 h, then placed them into a high temperature, oxygen-deficient oven by introducing  $N_2$  gas. The oven was kept at 450 °C for 2 h to carbonize the pistachio shells into char. The carbonization yield was 32.0 wt%.

Char was ground and sieved into a particle size ranging from 0.833 to 1.65 mm. The activation step was conducted by adding the char and NaOH in water, uniformly mixed, and dried at 130 °C. The solid was then placed in an oven that was heated and maintained at 780 °C for 1 h in the presence of  $N_2$  gas. The product was neutralized by HCl (600 cm<sup>3</sup>) having an equal equivalent to NaOH solution until most of  $CO_2$  bubbles were disappeared. The product was kept at 80 °C for 1 h in water bath, and washed continuously with distilled water till the water was neutral. The samples were classified according to agent/char ratio as PSN2, PSN2.5, PSN3 and PSN3.5. The first two characters, PS, represent the Pistachio shells. The third character, N, represents NaOH activation. The number represents the weight NaOH/char ratio.

The BET surface area of the adsorbent ( $S_p$ ) was measured from  $N_2$  adsorption isotherms at 77 K with a sorptiometer (Porous Materi-

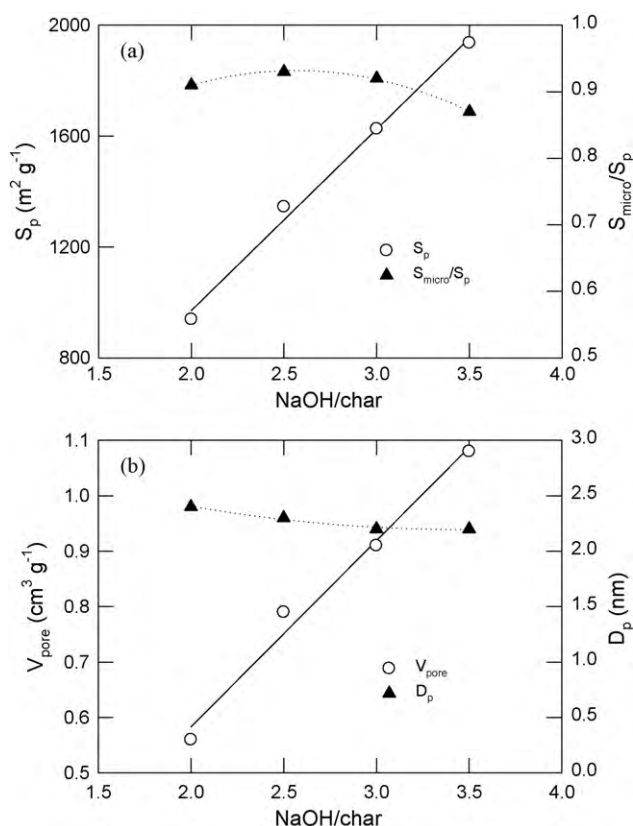


**Fig. 2.** (a) BET surface area and micropore surface area ratio, (b) total pore volume and mean pore diameter of activated carbon derived from pistachio shell by NaOH activation.

als Co., BET-202A), and the total pore volume ( $V_{pore}$ ) was calculated using the manufacturer's software. The pore size distribution was also determined using the BJH theory [50]. On the other hand, the micropore volume ( $V_{micro}$ ) and exterior surface area ( $S_{ext}$ ) were calculated by the  $t$ -plot method [51,52] and, accordingly, the micropore surface area ( $S_{micro}$ ) was obtained by subtracting  $S_{ext}$  from  $S_p$  [53].

### 3.2. Procedures for adsorption experiments

Analytical reagent grade acid blue 74 (AB74, Mw (molecular weight) = 466.4), basic brown 1 (BB1, Mw = 419.4), and methylene blue (MB, Mw = 284.3) were offered from Merck Co. and were used as received.

**Table 1**

Analysis of adsorptions of dyes on the activated carbons based on Langmuir and Freundlich equations.

Dyes	Carbon	Langmuir eq.			Freundlich eq.				
		$q_{mon}$ (g/kg)	$K_L$ ( $m^3/g$ )	$r^2$	$\Delta q_e$ (%)	$K_F^*$	$1/n$	$r^2$	$\Delta q_e$ (%)
BB1	PSN2	794	0.015	0.9982	2.98	182	0.217	0.970	2.85
	PSN2.5	1217	0.073	0.9995	6.20	429	0.181	0.926	15.7
	PSN3	1422	0.132	0.9998	5.90	531	0.186	0.864	11.4
	PSN3.5	1806	0.080	0.9981	8.83	413	0.298	0.954	8.02
MB	PSN2	394	0.029	0.9975	6.25	216	0.085	0.880	2.16
	PSN2.5	674	0.116	0.9996	25.1	410	0.081	0.989	1.25
	PSN3	745	0.218	0.9999	7.72	437	0.094	0.902	4.87
	PSN3.5	759	0.271	0.9999	14.3	474	0.099	0.880	6.56
AB74	PSN2	204	0.078	0.9996	2.63	116	0.093	0.995	0.45
	PSN2.5	465	0.052	0.9972	9.59	119	0.250	0.990	2.43
	PSN3	515	0.053	0.9979	2.77	115	0.283	0.953	5.80
	PSN3.5	574	0.068	0.9991	3.19	131	0.294	0.948	6.68

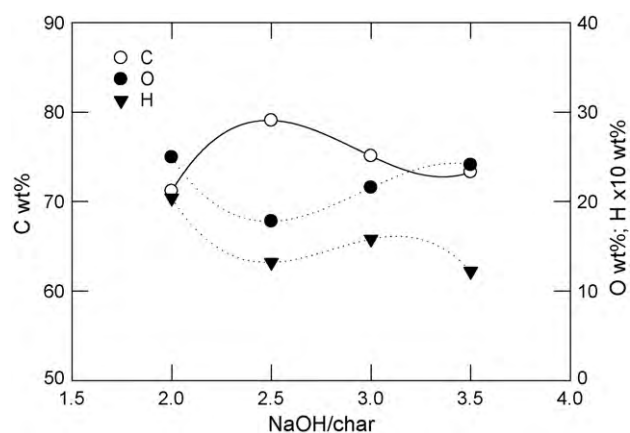


**Fig. 3.** Chemical compositions of activated carbon derived from pistachio shell by NaOH activation.

In the adsorption equilibrium experiments, an amount of the activated carbons (0.1 g) and 0.1 dm<sup>3</sup> of an aqueous phase were placed in a 0.25-dm<sup>3</sup> flask and stirred for 4 days in a water bath (Haake Model K-F3) at 30 °C. Preliminary tests showed that adsorption was complete after 3 days. The aqueous solution was prepared by dissolving solute to required concentration without pH adjustment. The molecular structures of MB, BB1, and AB74 have been described earlier [54]. The procedures for measuring adsorption isotherms and rates were identical to those described previously [55]. The concentrations of MB, AB74, and BB1 were determined with a Hitachi UV/visible spectrophotometer (U-2001). Each experiment was repeated at least three times under identical conditions. The amount of adsorption at equilibrium,  $q_e$  ( $g kg^{-1}$ ), was calculated by

$$q_e = \left( \frac{C_0 - C_e}{W} \right) V \quad (9)$$

where  $C_0$  and  $C_e$  are the initial and equilibrium liquid concentrations ( $g m^{-3}$ );  $V$  is the volume of the solution ( $m^3$ ); and  $W$  is the weight of dried carbons used (kg).

In order to compare the validity of two isotherm equations, a normalized standard deviation  $\Delta q_e$  (%) is calculated,

$$\Delta q_e (\%) = 100 \sqrt{\frac{\sum [(q_{e,exp} - q_{e,cat})/q_{e,exp}]^2}{N - 1}} \quad (10)$$

where  $N$  is the number of data.

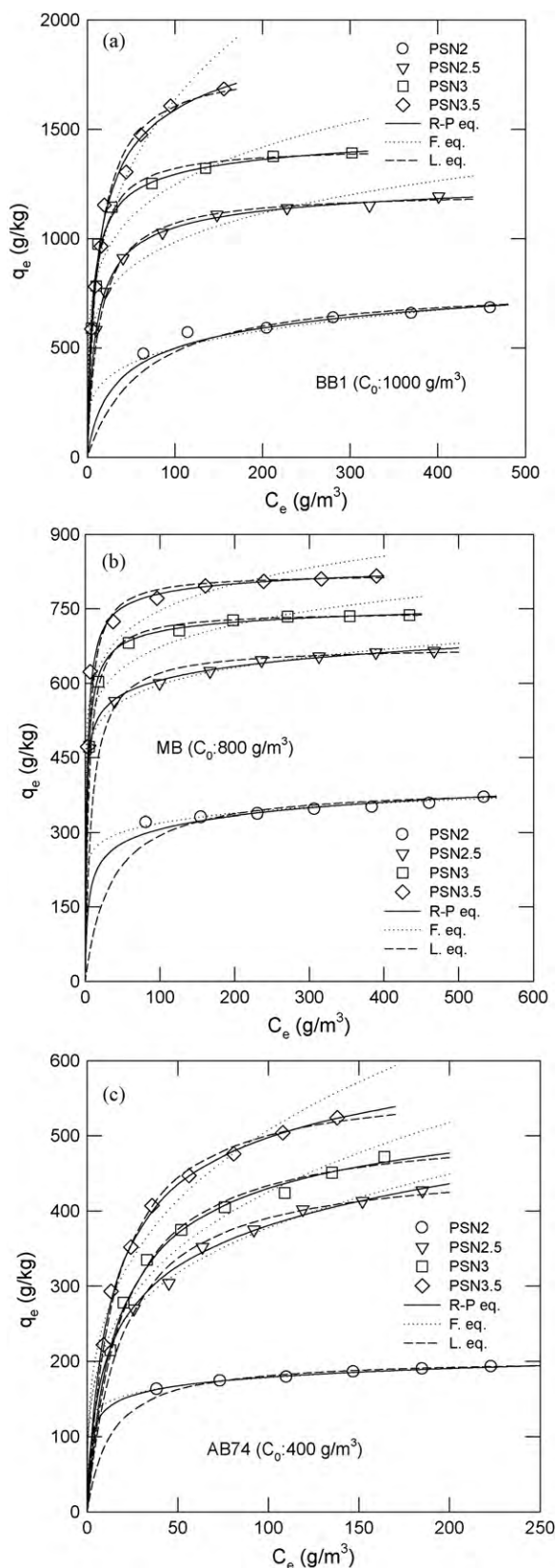


Fig. 4. Adsorption isotherm equilibrium of (a) BB1, (b) MB, and (c) AB74 at 30 °C on the activated carbons (PSN2 (○), PSN2.5 (▽), PSN3 (□), and PSN3.5 (◇), respectively).

## 4. Results and discussion

### 4.1. Properties of the activated carbons

This work prepared activated carbons from pistachio shells with NaOH at various NaOH/char ratios. Fig. 2(a) shows the relationships between BET specific surface area ( $S_p$ ) and micropore surface area ratio ( $S_{micro}/S_p$ ) and NaOH/char ratios. The data reveals that  $S_p$  increases with increased NaOH/char ratio, from 939 to 1936 m<sup>2</sup> g<sup>-1</sup>.  $S_{micro}/S_p$  values are between 0.87 and 0.93, a small variation. Fig. 2(b) shows the relationship between total pore volume ( $V_{pore}$ ) and mean pore size ( $D_p$ ) and NaOH/char ratios which reveals that  $V_{pore}$  increases with NaOH/char ratio, from 0.56 to 1.08 cm<sup>3</sup> g<sup>-1</sup>.  $D_p$  values are between 2.2 and 2.4 nm.

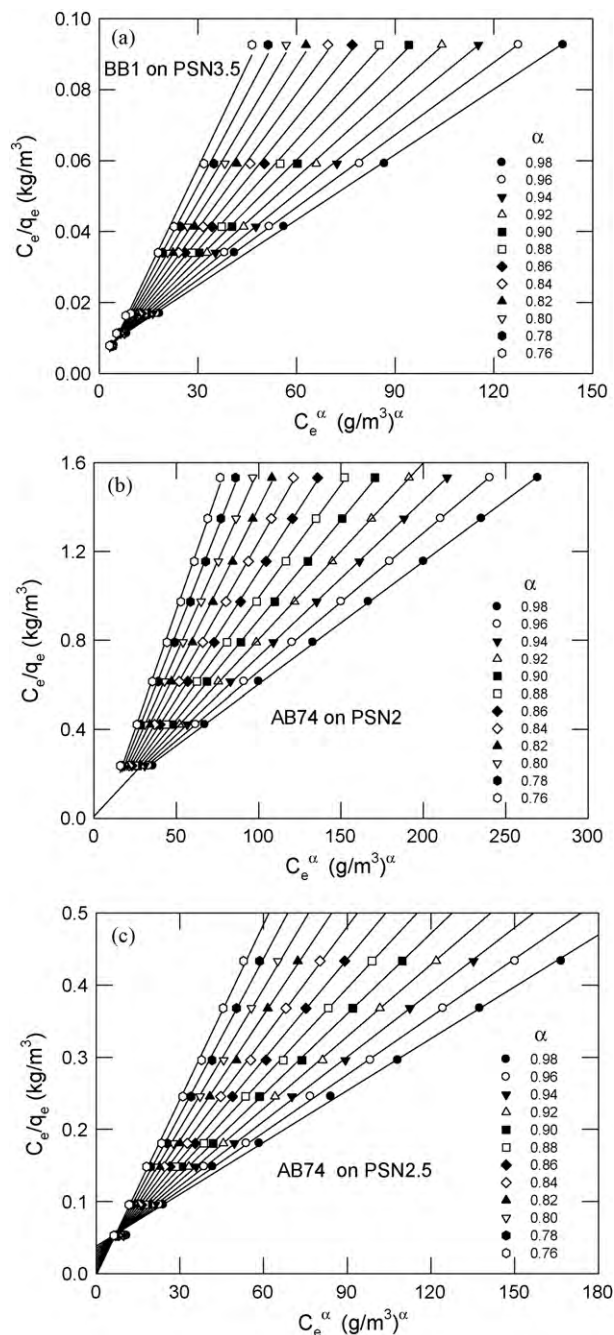


Fig. 5. Adsorption of (a) BB1 on PSN3.5, (b) AB74 on PSN2, (c) AB74 on PSN2.5 fitted with new linear form of Redlich–Peterson isotherm equation.



**Table 2**  
Analysis of adsorptions of dyes on the activated carbons based on Redlich–Peterson equations.

Dyes	Carbon	$q_{mon}$	$b_{RP} (m^3/g)^\alpha$	$\alpha$	$r^2$	$\Delta q_e (%)$
BB1	PSN2	351	0.079	0.88	0.9993	1.79
	PSN2.5	953	0.134	0.96	0.9998	0.30
	PSN3	1130	0.244	0.96	0.9999	4.81
	PSN3.5	1194	0.169	0.92	0.9990	4.23
MB	PSN2	200	0.505	0.90	0.9975	1.88
	PSN2.5	463	1.912	0.94	0.9999	0.65
	PSN3	658	0.442	0.98	1.0000	0.86
	PSN3.5	728	0.469	0.98	1.0000	4.80
AB74	PSN2	126	1.031	0.92	1.0000	0.42
	PSN2.5	173	0.541	0.82	0.9991	2.16
	PSN3	373	0.092	0.94	0.9988	2.01
	PSN3.5	380	0.141	0.92	0.9997	2.58

BB1:  $C_{max} = 500 \text{ g m}^{-3}$ , MB:  $C_{max} = 700 \text{ g m}^{-3}$ , AB74:  $C_{max} = 400 \text{ g m}^{-3}$ .

Analyzed elements [56,57] express the chemical properties of activated carbon prepared with chemical activation. Fig. 3 lists weight percents of C, O, and H of the activated carbons studied. Element C is 71–79 wt%; O, 18–25 wt%; H, 1.2–2.0 wt%.

#### 4.2. Adsorption equilibrium of dyes and three isotherm equations

This isotherm equilibrium adsorption study used three dyes (BB1, MB, and AB74) as adsorbates and PSN2, PSN2.5, PSN3, and PSN3.5, the activated carbons of activated at different NaOH/char ratios, as adsorbents. Fig. 4(a)–(c) shows the experiment data results. Data were fitted with Langmuir and Freundlich isotherm equations, and the results summarized in Table 1. Table 1 shows that  $r^2$  values of the Langmuir isotherm equation are larger than 0.9972. However,  $\Delta q_e (%)$  values are widely distributed, from 2.63%

to 25.1%. This study excellently fitted the Freundlich isotherm equation to the experimental data of the adsorption systems of MB and AB74 on PSN2 and PSN2.5 with very small deviation values.

To fit the R–P isotherm equation to experimental data set, the linear regression lines were constructed by plotting  $C_e/q_e$  vs.  $C_e^\alpha$  of Eq. (3) with various  $\alpha$  values. In this paper, first, the value of  $C_e^\alpha$  was calculated for each  $\alpha$  value, and then the linear regression line associated with this specific  $\alpha$  value was plotted.

Fig. 5(a)–(c) shows three families of regression lines for the adsorption systems of BB1 on PSN3.5, AB74 on PSN2, and AB74 on PSN2.5, respectively. The  $\alpha$  values of the most suitable linear regression lines are, respectively, 0.92, 0.92, and 0.82. The intercepts of straight lines are all close to 0 for all  $\alpha$  values. Table 2 lists the obtained values of  $q_{mon}$ ,  $b_{RP}$ ,  $\alpha$ ,  $r^2$ , and  $\Delta q_e (%)$ . All the  $r^2$  values are larger than 0.9988 and all the  $\Delta q_e (%)$  values are less

**Table 3**  
Redlich–Peterson and Langmuir isotherm equations of the adsorption of dyes obtained from the literature.

No.	Dyes	Adsorbent	Redlich–Peterson eq.			Langmuir eq. $q_{mon} (\text{g/kg})$	Ref.
			$\alpha$	$b_{RP} (m^3 g^{-1})^\alpha$	$q_{mon}$		
1	Malachite G	AC	1.00	0.0198	510	509	[32]
2	RR	Silica	1.00	0.012	16.1	16.2	[60]
3	MB	Lemon peel	1.00	0.0558	33.2	33.2	[61]
4	MB	AC	1.00	0.0442	401	401	[33]
5	RY	FS400	0.99	0.28	700	714	[16]
6	RB19	CC/OPA	0.965	0.04	434	667	[11]
7	BlueG	Beet pulp	0.96	0.020	194	250	[41]
8	MB	Red mud	0.949	0.261	1.93	2.64	[9]
9	BG	RHA	0.939	2.10	19.5	26.2	[34]
10	RR	FS400	0.93	0.02	180	213	[16]
11	Blue-G	Fungus	0.925	0.014	502	601	[62]
12	BB3	Peat	0.914	0.327	324	556	[8]
13	RR	Silica	0.91	0.184	15.9	24.1	[60]
14	RB	FS400	0.91	0.10	168	278	[16]
15	Blue-G	Fungus	0.901	0.16	324	555	[62]
16	Malachite G	Biomass	0.894	0.142	78.9	118	[31]
17	BY21	Peat	0.887	0.121	355	667	[8]
18	AR	AC	0.868	1.20	58.6	101	[24]
19	AB	AC	0.866	17.2	61.9	101	[24]
20	BR22	Peat	0.865	0.996	128	312	[8]
21	MV	BFA	0.861	2.35	17.5	26.2	[19]
22	BR22	Kudzu	0.843	0.293	69.8	192	[62]
23	AY	AC	0.825	32.89	74.3	129	[24]
24	MB	Fibres	0.74	0.77	2.48	5.56	[64]
25	MV	WC	0.677	0.71	38.4	240	[25]
26	AR	WC	0.657	1.93	35.4	246	[25]
27	CR	WC	0.648	0.35	31.9	234	[25]
28	OG	WC	0.602	0.66	25.9	236	[25]
29	Malachite G	ACL	0.618	3.29	7.36	42.2	[65]
30	Malachite G	ACC	0.597	68.6	1.21	8.27	[63]
31	Malachite G	BFA	0.583	89.2	25.5	170	[65]
32	RB	Alga	0.53	0.36	16.2	357	[57]
33	RB	Alga	0.48	0.51	17.6	476	[59]
34	OG	MV	0.458	182	3.10	26.2	[19]
35	RB19	CC/OPA	0.188	0.414	53.9	909	[11]

than those listed in Table 1 of the fitted Langmuir and Freundlich isotherm equations. Tables 1 and 2 show that  $\Delta q_e$  (%) values of MB adsorption on PSN2.5 are, respectively, 25.1%, 1.25%, and 0.65% for Langmuir, Freundlich, and R–P isotherm equations. The Freundlich, and R–P isotherm equations are much more suitable than the Langmuir equation in fitting to the data set of MB adsorption on PSN2.5. The value of  $b_{RP}$  in the R–P isotherm equation is high, up to 1.912, for MB adsorption on PSN2.5, much higher than 0.079–0.244 for BB1 adsorption as shown in Table 2. Fig. 4(a)–(c) shows the calculated curves of three isotherm equations and that the curvatures of the curves of the R–P equation are higher than those of the Freundlich equation but lower than those of the Langmuir equation. All  $\alpha$  values were less than 1 (see explanation of Fig. 1), from 0.82 to 0.98 as listed in Table 2.

Table 3 lists thirty-five adsorption systems of dyes fitted with the R–P isotherm equation. Among them, four systems have an  $\alpha$  value of 1 and the rest have an  $\alpha$  value less than 1. Large molecule adsorption, as in dyes, is not easy in accordance with the theory of monolayer adsorption upon which the Langmuir isotherm equation is based. This is because impediments exist between pores and adsorbate so the  $\alpha$  value is usually less than 1.

In a report of dye adsorptions on chitosan [14], the Langmuir isotherm equation was better fitted to the adsorptions of AG25, AR18, AR73, AO12. The Freundlich isotherm equation was better fitted to the adsorption of AO10 and the R–P isotherm equation to those of all dyes with the lowest error values. In a report of basic dye adsorption on kudzu [58], the error values of Freundlich and R–P isotherm equations in fitting to the adsorption of BY21 were both the same and the least. The error value of the R–P isotherm equation in fitting to the adsorption of BR22 was the least. In a report of reactive dye adsorption on green alga [59], the errors of Freundlich and R–P isotherm equations in fitting to RBB adsorption were both the same and the least. Consequently, the above reports show that error values of the R–P isotherm equation are either close to those of the Freundlich or the Langmuir equations, or less than those of both equations. These findings agree with the results of this study.

## 5. Conclusions

This study explains the special conditions of the R–P isotherm equation and proves they are in accordance with Langmuir and Freundlich isotherm equations. Thus the R–P isotherm equation is suitable for wide applications. This investigation deduces the dimensionless form of the R–P isotherm equation and plots curves of the dimensionless form. The current study explains that the  $\alpha$  value modifies R–P isotherm equation curves. Microporous activated carbons with BET specific surface area ( $S_p$ ) from 939 to 1936 m<sup>2</sup> g<sup>-1</sup> were prepared from pistachio shells with NaOH activation for the adsorptions of three dyes (AB74, BB1, and MB). The linear regressions calculated are used to identify the most suitable  $\alpha$  value. This is a simple and accurate calculation method. In fitting the data sets of the adsorptions of three dyes, the R–P isotherm equation is the best with  $\alpha$  values being between 0.82 and 0.98. This investigation employed thirty-five adsorption systems of dyes reported in the literature to explain the existence of a solid impediment between pores and adsorbate, so the  $\alpha$  value is usually less than 1 in the adsorption of large molecules.

## Acknowledgments

Financial support of this work by the National Science Council of the Republic of China under contract no. NSC 97-2221-E-239-016 is gratefully acknowledged.

## References

- [1] O. Redlich, D.L. Peterson, A useful adsorption isotherm, *J. Phys. Chem.* 63 (1959) 1024–1026.
- [2] N. Haimour, R. El-Bishtawi, A. Ail-Wahbi, Equilibrium adsorption of hydrogen sulfide onto CuO and ZnO, *Desalination* 181 (2005) 145–152.
- [3] Z. Aksu, D. Akpinar, Modelling of simultaneous biosorption of phenol and nickel(II) onto dried aerobic activated sludge, *Sep. Purif. Technol.* 21 (2000) 87–99.
- [4] M.S. Bilgili, Adsorption of 4-chlorophenol from aqueous solutions by xad-4 resin: Isotherm, kinetic, and thermodynamic analysis, *J. Hazard. Mater.* 137 (2006) 157–164.
- [5] A. Benhammou, A. Yaacoubi, L. Nibou, B. Tanouti, Adsorption of metal ions onto Moroccan stevensite: kinetic and isotherm studies, *J. Colloid Interface Sci.* 282 (2005) 320–326.
- [6] E.N. El Qada, S.J. Allen, G.M. Walker, Adsorption of Methylene Blue onto activated carbon produced from steam activated bituminous coal: a study of equilibrium adsorption isotherm, *Chem. Eng. J.* 124 (2006) 103–110.
- [7] V.C. Srivastava, M.M. Swamy, I.D. Mall, B. Prasad, I.M. Mishra, Adsorptive removal of phenol by bagasse fly ash and activated carbon: equilibrium, kinetics and thermodynamics, *Colloid Surf.* 272 (2006) 89–104.
- [8] S.J. Allen, G. McKay, J.F. Porter, Adsorption isotherm models for basic dye adsorption by peat in single and binary component systems, *J. Colloid Interface Sci.* 280 (2004) 322–333.
- [9] S. Wang, Y. Boyjoo, A. Choueb, Z.H. Zhu, Removal of dyes from aqueous solution using fly ash and red mud, *Water Res.* 39 (2005) 129–138.
- [10] W.T. Tsai, H.C. Hsu, T.Y. Su, K.Y. Lin, C.M. Lin, T.Y. Hsu, K.Y. Su, C.M. Lin, Lin, Adsorption characteristics of bisphenol-A in aqueous solutions onto hydrophobic zeolite, *J. Colloid Interface Sci.* 299 (2006) 513–519.
- [11] M. Hasan, A.L. Ahmad, B.H. Hameed, Adsorption of reactive dye onto cross-linked chitosan/oil palm ash composite beads, *Chem. Eng. J.* 136 (2008) 164–172.
- [12] A. Artola, M. Martin, M. Balaguer, M. Rigola, Isotherm model analysis for the adsorption of Cd (II), Cu (II), Ni (II), and Zn (II) on anaerobically digested sludge, *J. Colloid Interface Sci.* 232 (2000) 64–70.
- [13] Z. Aksu, J. Yener, A comparative adsorption/biosorption study of monochlorinated phenols onto various sorbents, *Waste Manage* 21 (2001) 695–702.
- [14] A. Gunay, E. Arslankaya, I. Tosun, Lead removal from aqueous solution by natural and pretreated clinoptilolite: adsorption equilibrium and kinetics, *J. Hazard. Mater.* 146 (2007) 362–371.
- [15] J.P. Wang, Y.Z. Chen, H.M. Feng, S.J. Zhang, H.Q. Yu, Removal of 2,4-dichlorophenol from aqueous solution by static-air-activated carbon fibers, *J. Colloid Interface Sci.* 313 (2007) 80–85.
- [16] Y. Al-Degs, M.A.M. Khraisheh, S.J. Allen, M.N. Ahmad, G.M. Walker, Competitive adsorption of reactive dyes from solution: Equilibrium isotherm studies in single and multicomponent systems, *Chem. Eng. J.* 128 (2007) 163–167.
- [17] S. Debnath, U.C. Ghosh, Kinetics, isotherm and thermodynamics for Cr(III) and Cr(VI) adsorption from aqueous solutions by crystalline hydrous titanium oxide, *J. Chem. Thermodyn.* 40 (2008) 67–77.
- [18] V.C. Srivastava, I.D. Mall, I.M. Mishra, Removal of cadmium(II) and zinc(II) metal ions from binary aqueous solution by rice husk ash, *Colloids Surf. A: Physicochem. Eng. Aspects* 312 (2008) 172–184.
- [19] I.D. Mall, V.C. Srivastava, N.K. Agarwal, Removal of Orange-G and Methyl Violet dyes by adsorption onto bagasse fly ash—kinetic study and equilibrium isotherm analyses, *Dye Pigment* 69 (2006) 210–223.
- [20] L. Zeng, X. Li, J. Liu, Adsorptive removal of phosphate from aqueous solutions using iron oxide tailings, *Water Res.* 38 (2004) 1318–1326.
- [21] Z. Aksu, O. Tunc, Application of biosorption for penicillin G removal: comparison with activated carbon, *Process Biochem.* 40 (2005) 831–847.
- [22] P.A.M. Mourao, P.J.M. Carrott, M.M.L. Ribeiro Carrott, Application of different equations to adsorption isotherms of phenolic compounds on activated carbons prepared from cork, *Carbon* 44 (2006) 2422–2429.
- [23] A. Ozer, G. Akkaya, M. Turabik, The biosorption of Acid Red 337 and Acid Blue 324 on *Enteromorpha prolifera*: the application of nonlinear regression analysis to dye biosorption, *Chem. Eng. J.* 112 (2005) 181–190.
- [24] K.K.H. Choy, G. McKay, J.F. Porter, Sorption of acid dyes from effluents using activated carbon, *Resour. Conserv. Recycl.* 27 (1999) 57–71.
- [25] I.D. Mall, V.C. Srivastava, G.V.A. Kumar, I.M. Mishra, Characterization and utilization of mesoporous fertilizer plant waste carbon for adsorptive removal of dyes from aqueous solution, *Colloid Surf.* A278 (2006) 175–187.
- [26] F.A. Pavan, S.L.P. Dias, E.C. Lima, E.V. Benvenuti, Removal of Congo red from aqueous solution by anilinepropylsilica xerogel, *Dye Pigment* 76 (2008) 64–69.
- [27] M. Arami, N.Y. Limaee, N.M. Mahmoodi, Investigation on the adsorption capability of egg shell membrane towards model textile dyes, *Chemosphere* 65 (2006) 1999–2008.
- [28] Y.S. Ho, A.E. Ofomaja, Kinetics and thermodynamics of lead ion sorption on palm kernel fibre from aqueous solution, *Process Biochem.* 40 (2005) 3455–3461.
- [29] B.S. Inbaraj, C.P. Chiu, G.H. Ho, J. Yang, B.H. Chen, Removal of cationic dyes from aqueous solution using an anionic poly- $\gamma$ -glutamic acid-based adsorbent, *J. Hazard. Mater.* 137 (2006) 226–234.
- [30] V. Padmavathy, Biosorption of nickel (II) ions by baker's yeast: kinetic, thermodynamic and desorption studies, *Bioresour. Technol.* 99 (2008) 3100–3109.
- [31] K.V. Kumar, S. Sivanesan, V. Ramamurthi, Adsorption of malachite green onto *Pithophora* sp., a fresh water algae: equilibrium and kinetic modeling, *Process Biochem.* 40 (2005) 2865–2872.

- [32] K.V. Kumar, Comparative analysis of linear and non-linear method of estimating the sorption isotherm parameters for malachite green onto activated carbon, *J. Hazard. Mater.* 136 (2006) 197–202.
- [33] K.V. Kumar, S. Sivanesan, Equilibrium data, isotherm parameters and process design for partial and complete isotherm of methylene blue onto activated carbon, *J. Hazard. Mater.* 134 (2006) 237–244.
- [34] V.S. Mane, I. Deo Mall, V. Chandra Srivastava, Kinetic and equilibrium isotherm studies for the adsorptive removal of Brilliant Green dye from aqueous solution by rice husk ash, *J. Environ. Manage.* 84 (2007) 390–400.
- [35] K.V. Kumar, K. Porkodi, Batch adsorber design for different solution volume/adsorbent mass ratios using the experimental equilibrium data with fixed solution volume/adsorbent mass ratio of malachite green onto orange peel, *Dye Pigment* 74 (2007) 590–594.
- [36] R. Han, Z. Lu, W. Zou, W. Daotong, J. Shi, Y. Jiujun, Removal of copper(II) and lead(II) from aqueous solution by manganese oxide coated sand. II. Equilibrium study and competitive adsorption, *J. Hazard. Mater.* 137 (2006) 480–488.
- [37] Y.S. Ho, A.E. Ofomaja, Biosorption thermodynamics of cadmium on coconut copra meal as biosorbent, *Biochem. Eng. J.* 30 (2006) 117–123.
- [38] K.V. Kumar, Optimum sorption isotherm by linear and non-linear methods for malachite green onto lemon peel, *Dye Pigment* 74 (2007) 595–597.
- [39] B.S. Inbaraj, N. Sulochana, Mercury adsorption on a carbon sorbent derived from fruit shell of *Terminalia catappa*, *J. Hazard. Mater.* 133 (2006) 283–290.
- [40] Z. Aksu, H. Gulen, Binary biosorption of iron(III) and iron(III)-cyanide complex ions on *Rhizopus arrhizus*: modelling of synergistic interaction, *Process Biochem.* 38 (2002) 161–173.
- [41] Z. Aksu, I.A. Isoglu, Use of agricultural waste sugar beet pulp for the removal of Gemazol turquoise blue-G reactive dye from aqueous solution, *J. Hazard. Mater.* 137 (2006) 418–430.
- [42] K. Porkodi, K.V. Kumar, Equilibrium, kinetics and mechanism modeling and simulation of basic and acid dyes sorption onto jute fiber carbon: Eosin yellow, malachite green and crystal violet single component systems, *J. Hazard. Mater.* 143 (2007) 311–327.
- [43] K.V. Kumar, S. Sivanesan, Pseudo second order kinetics and pseudo isotherms for malachite green onto activated carbon: comparison of linear and non-linear regression methods, *J. Hazard. Mater.* 136 (2006) 721–726.
- [44] A. Verma, S. Chakraborty, J.K. Basu, Adsorption study of hexavalent chromium using tamarind hull-based adsorbents, *Sep. Purif. Technol.* 50 (2006) 336–341.
- [45] Z. Aksu, D. Akpınar, Competitive biosorption of phenol and chromium (VI) from binary mixtures onto dried anaerobic activated sludge, *Biochem. Eng. J.* 7 (2001) 183–193.
- [46] B. Preetha, T. Viruthagiri, Batch and continuous biosorption of chromium(VI) by *Rhizopus arrhizus*, *Sep. Purif. Technol.* 57 (2007) 126–133.
- [47] H. Yavuz, A. Denizli, H. Gungunes, M. Safarikova, I. Safarik, Biosorption of mercury on magnetically modified yeast cells, *Sep. Purif. Technol.* 52 (2006) 253–260.
- [48] M. Ahmaruzzaman, D.K. Sharma, Adsorption of phenols from wastewater, *J. Colloid Interface Sci.* 287 (2005) 14–24.
- [49] V.M. Boddu, K. Abburi, J.L. Talbott, E.D. Smith, R. Haasch, Removal of arsenic (III) and arsenic (V) from aqueous medium using chitosan-coated biosorbent, *Water Res.* 42 (2008) 633–642.
- [50] E.P. Barrett, L.G. Joyner, P.P. Halenda, The determination of pore volume and area distribution in porous substances. I. Computation from nitrogen isotherms, *J. Am. Chem. Soc.* 73 (1951) 373–380.
- [51] J.H. de Boer, B.C. Lippens, B.G. Linsen, J.C.P. Broekhoff, A. van den Heuvel, T.J. Osiga, The *t*-curve of multimolecular N<sub>2</sub>-adsorption, *J. Colloid Interface Sci.* 21 (1966) 405–414.
- [52] K.S.W. Sing, D.H. Everett, R.A.W. Haul, L. Moscou, R.A. Pierotti, J. Rouquerol, Reporting physisorption data for gas/solid systems with special reference to the determination of surface area and porosity, *Pure Appl. Chem.* 57 (1985) 603–619.
- [53] E.F. Sousa-Aguilar, A. Liebsch, B.C. Chaves, A.F. Costa, Influence of external surface area of small cryatallite zeolites on the micropore volume determination, *Microporous Mesoporous Mater.* 25 (1998) 185–192.
- [54] F.C. Wu, R.L. Tseng, C.C. Hu, Comparisons of properties and adsorption performance of KOH-activated and steam-activated carbons, *Microporous Mesoporous Mater.* 80 (2005) 95–106.
- [55] F.C. Wu, R.L. Tseng, R.S. Juang, Comparisons of porous and adsorption properties of carbons activated by steam and KOH, *J. Colloid Interface Sci.* 283 (2005) 49–56.
- [56] R.L. Tseng, Physical and chemical properties and adsorption type of activated carbon prepared from plum kernels by NaOH activation, *J. Hazard. Mater.* 147 (2007) 1020–1027.
- [57] R.L. Tseng, S.K. Tseng, F.C. Wu, C.C. Hu, C.C. Wang, Effects of micropore development on the physicochemical properties of KOH-activated carbons, *J. Chin. Inst. Chem. Eng.* 39 (2008) 37–47.
- [58] J.C.Y. Ng, W.H. Cheung, G. McKay, Equilibrium studies for the sorption of lead from effluents using chitosan, *Chemosphere* 52 (2003) 1021–1030.
- [59] Z. Aksu, S. Tezer, Biosorption of reactive dyes on the green alga *Chlorella vulgaris*, *Process Biochem.* 40 (2005) 1347–1361.
- [60] A.R. Cestari, E.F.S. Vieira, G.S. Vieira, L.E. Almeida, Aggregation and adsorption of reactive dyes in the presence of an anionic surfactant on mesoporous aminopropyl silica, *J. Colloid Interface Sci.* 309 (2007) 402–411.
- [61] K.V. Kumar, K. Porkodi, Relation between some two- and three-parameter isotherm models for the sorption of methylene blue onto lemon peel, *J. Hazard. Mater.* 138 (2006) 633–635.
- [62] Z. Aksu, S.S. Cagatay, Investigation of biosorption of Gemazol Turquoise Blue-G reactive dye by dried *Rhizopus arrhizus* in batch and continuous systems, *Sep. Purif. Technol.* 48 (2006) 24–35.
- [63] S.J. Allen, Q. Gan, R. Matthews, P.A. Johnson, Comparison of optimised isotherm models for basic dye adsorption by kudzu, *Bioresour. Technol.* 88 (2003) 143–152.
- [64] M.C. Ncibi, B. Mahjoub, M. Seffen, Kinetic and equilibrium studies of methylene blue biosorption by *Posidonia oceanica* (L.) fibres, *J. Hazard. Mater.* 139 (2007) 280–285.
- [65] I.D. Mall, V.C. Srivastva, N.K. Agarwal, I.M. Mishra, Adsorptive removal of malachite green dye from aqueous solution by bagasse fly ash and activated carbon-kinetic study and equilibrium isotherm analyses, *Colloid Surf. A264* (2005) 17–28.